A&A 380, L31–L34 (2001)
DOI: 10.1051/0004-6361:20011510
© ESO 2001

Astronomy & Astrophysics

Letter to the Editor

Temporal properties of the short gamma-ray bursts

S. McBreen[1], F. Quilligan[1], B. McBreen[1], L. Hanlon[1], and D. Watson[2]

[1] Department of Experimental Physics, University College Dublin, Dublin 4, Ireland
[2] X-Ray Astronomy Group, Department of Physics and Astronomy, Leicester University, Leicester LE1 7RH, UK

Received 29 August 2001 / Accepted 22 October 2001

Abstract. A temporal analysis has been performed on a sample of 100 bright gamma-ray bursts (GRBs) with $T_{90} < 2$ s from the BATSE Current Catalog. The GRBs were denoised using a median filter and subjected to an automated pulse selection algorithm as an objective way of identifing the effects of neighbouring pulses. The rise times, fall times, $FWHM$, pulse amplitudes and areas were measured and the frequency distributions are presented here. All are consistent with lognormal distributions. The distribution of time intervals between pulses is not random but consistent with a lognormal distribution. The time intervals between pulses and pulse amplitudes are highly correlated with each other. These results are in excellent agreement with a similar analysis that revealed lognormal distributions for pulse properties and correlated time intervals between pulses in bright GRBs with $T_{90} > 2$ s. The two sub-classes of GRBs appear to have the same emission mechanism which is probably caused by internal shocks. They may not have the same progenitors because of the generic nature of the fireball model.

Key words. gamma-rays – bursts: gamma-rays – observations: methods – data analysis: methods – statistical

1. Introduction

It has been recognised that GRBs may occur in two sub-classes based on spectral hardness and duration with $T_{90} > 2$ s and $T_{90} < 2$ s (Kouveliotou et al. 1993; Dezalay et al. 1995; Paciesas et al. 2001). The bimodal distribution can be fit by two Gaussian distributions in the logarithmic durations (McBreen et al. 1994). There is significant evidence for a third subgroup as part of the long duration GRBs (Mukherjee et al. 1998; Horvath 1998) but this has been questioned because of a possible BATSE selection effect (Hakkila et al. 2000). It has been suggested (Cline et al. 1999) that the small group of GRBs with $T_{90} <$ 0.1 s form an additional category. The short GRBs have a higher value of $\langle V/V_{\max}\rangle$ (Katz & Canel 1996), a much smaller value of the spectral lag (Norris et al. 2000), a pulse shape that depends on position in the burst (Gupta et al. 2000) and a smaller space density than long GRBs (Schmidt 2001).

A variety of statistical methods have been applied to the temporal properties of GRBs with $T_{90} > 2$ s. It is important to compare the temporal profiles of the long and short GRBs to determine the similarities and differences between the two classes in an objective way. A detailed objective analysis has been performed on the temporal profiles of a large sample of 319 bright GRBs with $T_{90} > 2$ s (Quilligan et al. 2001; Hurley et al. 1998). The properties of the pulses in GRBs and the time intervals between them were found to be consistent with lognormal distributions. These results can be used as templates for comparison with a similar analysis of GRBs with $T_{90} < 2$ s.

The analysis method is presented in Sect. 2 and the results in Sect. 3. In Sect. 4 the results are discussed and compared with the sample of long GRBs.

Send offprint requests to: S. McBreen,
e-mail: smcbreen@bermuda.ucd.ie

2. Data preparation

The dataset was taken from the BATSE current catalog. The time tagged event data at 5 ms resolution was used. The data from the four energy channels were combined into a single channel to maximise the signal to noise ratio. A subset of the current catalogue was selected with GRB durations less than two seconds ($T_{90} < 2$ s). These GRBs were ordered according to their peak flux in 256 ms ($P_{256\mathrm{ms}}$) and the first 100 bursts without data gaps and with 5 ms data available for the complete burst where selected. All GRBs in the sample had $P_{256\mathrm{ms}} >$ 1.6 photons cm^{-2} s^{-1}.

2.1. Background subtraction

The first step in the data preparation involved selecting the appropriate background for subtraction. The start and end times for each burst were identified. A background section was then identified which was usually after the main section of the GRB. If 5 ms data was available for

Article published by EDP Sciences and available at http://www.aanda.org or http://dx.doi.org/10.1051/0004-6361:20011510

Table 1. The parameters of the pulse properties in GRBs include the median value for the data, the median μ and the standard deviation σ expressed as natural logarithms, the width of the lognormal distributions at the $\pm 50\%$ level in normal space, the KS probability that properties of pulses selected at different levels of τ_σ and $\tau_{\rm i}$ were drawn from the same distribution as those selected at $\tau_\sigma \geq 5$, $\tau_{\rm i} \geq 50\%$. All pulses with $\tau_\sigma \geq 5$ were used for the time intervals and not just isolated pulses. The values for the pulse areas and amplitudes were obtained from 55 GRBs that were summed over two BATSE Large Area Detectors.

Property	Median	μ	σ	Width ($\pm 50\%$)	KS ($\tau_\sigma \geq 3$,$\tau_{\rm i} \geq 20\%$)	KS ($\tau_\sigma \geq 8$, $\tau_{\rm i} \geq 80\%$)
Rise Time	0.035	−3.31	0.94	0.012–0.11	0.48	0.16
Fall Time	0.056	−2.89	0.98	0.017–0.176	0.07	0.19
$FWHM$	0.045	−3.17	1.01	0.013–0.138	0.73	0.48
Area	1.5×10^5	11.7	1.24	28–520 ($\times10^3$)	0.44	0.15
Pulse Amplitude	1.02×10^4	9.22	0.83	3.8–27 ($\times10^3$)	0.90	0.72
Asymmetry Ratio	0.65	−0.42	0.91	0.19–2.22	0.78	0.30
ΔT	0.095	−2.24	0.87	0.038–0.3	0.83	0.96

the background level estimation, it was used, otherwise a 64 ms section was selected. The median value of the data points in the background section was subtracted from all other values in the active section of the GRB.

2.2. Denoising and pulse selection

A median filter was used to denoise the GRBs. This denoises a signal by finding the median of each bin. The best denoised signal was found by varying the bin size and the value of σ. The wavelet method (Quilligan et al. 2001) was not used because the short durations of the GRBs produced a smaller number of data points than that required for our wavelet method.

The pulse selection method was described elsewhere (Quilligan et al. 2001). The pulses selected had a threshold of 5 σ ($\tau_\sigma \geq 5$) and isolated from adjacent pulses by at least 50% ($\tau_{\rm i} \geq 50\%$). A value of $\tau_{\rm i} \geq 50\%$ implies that the two minima on either side of the pulse maximum must be at or below half the maximum value. A total of 313 pulses were selected with $\tau_\sigma \geq 5$ and 181 of these had $\tau_{\rm i} \geq 50\%$.

3. Results

3.1. Distributions of $t_{\rm r}$, $t_{\rm f}$, FWHM, pulse area, pulse amplitude and ΔT

The distribution of the number of pulses with $\tau_\sigma \geq 5$ is given in Fig. 1. The median value of the number of pulses per GRB is 2.5 and is smaller than the value of 6 for long GRBs (Quilligan et al. 2001). The distributions of rise time $t_{\rm r}$, fall time $t_{\rm f}$ and full width at half maximum ($FWHM$) for the isolated pulses are presented in Fig. 2 along with the lognormal fits to the data. The distributions of pulse amplitudes and areas are presented in Fig. 3 for the isolated pulses. The distribution of time intervals between pulses with $\tau_\sigma \geq 5$ is given in Fig. 4.

The median values and the parameters of the lognormal fits are presented in Table 1. The distribution of the pulse asymmetry ratios, $t_{\rm r}/t_{\rm f}$, is not presented but the values are listed in Table 1. The pulse fall time is generally longer than the rise time. The widths or ranges of the lognormal distributions at the $\pm 50\%$ are are also given in Table 1. The Kolmogorov-Smirnov (KS) test was used to indicate the effects of varying τ_σ and $\tau_{\rm i}$. The pulse property distributions at $\tau_\sigma \geq 5$ and $\tau_{\rm i} \geq 50\%$ were compared with the distributions selected over large range of τ_σ and $\tau_{\rm i}$. The significance level probabilities from the KS test for the comparison are presented in Table 1 for $\tau_\sigma \geq 3$, $\tau_{\rm i} \geq 20\%$ and $\tau_\sigma \geq 8$, $\tau_{\rm i} \geq 80\%$ and all have acceptable values. It was found that when $\tau_{\rm i}$ increased the pulses become less contaminated by overlaps from adjacent pulses.

3.2. Correlation analysis

The correlation coefficients between a range of GRB parameters and pulse parameters were obtained using the Spearman Rank Order correlation coefficents ρ with associated probabilities and the values are listed in Table 2. The correlation coefficients for the time intervals between pulses are listed in Table 3 and they are strongly correlated with each other.

4. Discussion

The major result is that pulses in GRBs with $T_{90} < 2$ s have very similar distributions of $t_{\rm r}$, $t_{\rm f}$, $FWHM$, pulse

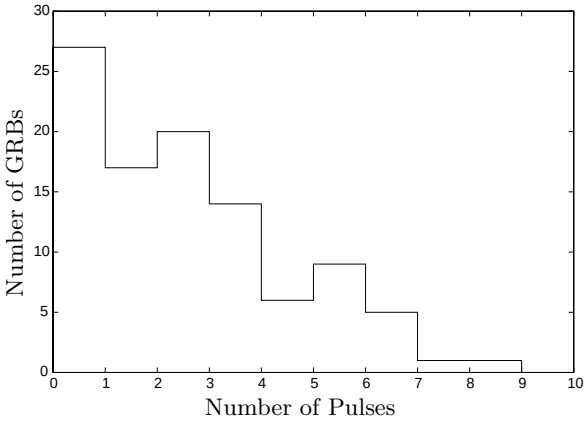

Fig. 1. The number of pulses versus number of γ-ray bursts.

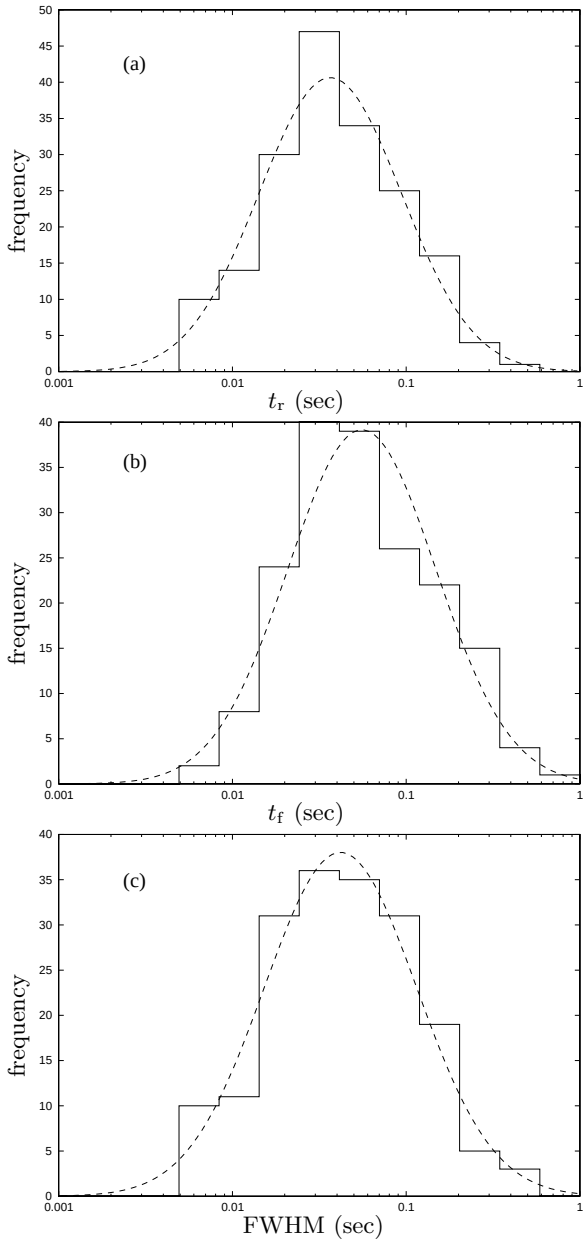

Fig. 2. The distribution of t_r, t_f, and $FWHM$ (**a**)–**c**)) for pulses with $\tau_\sigma \geq 5$ and $\tau_i \geq 50\%$. The dashed lines are lognormals that are consistent with the data.

amplitude, pulse area and ΔT. The frequency distributions are broad and all are compatible with lognormal distributions, and at the 50% level span an order of magnitude in the particular pulse property (Table 1). The same pulse properties in GRBs with $T_{90} > 2$ s are also well described by lognormal distributions (Quilligan et al. 2001). The results of the correlation analysis on the GRBs and the properties of the pulses (Table 2) are generally in good agreement between long and short GRBS. The main difference is the pulse amplitude because it is not anticorrelated with t_r, t_f and $FWHM$. In GRBs with $T_{90} > 2$ s the values of ΔT are not random but consistent with a lognormal distribution with a Pareto-Levy tail for a small

Table 2. Spearman Rank Order correlation coefficients ρ and associated probabilities between a range of burst (first 3 rows) and pulse parameters (second 10 rows).

Properties	ρ	Probability
No. of Pulses vs. T_{90}	0.18	0.073
No. of Pulses vs. Total Fluence	0.38	9.8×10^{-5}
T_{90} vs. Total Fluence	0.21	0.037
Rise Time vs. Fall Time	0.54	2.7×10^{-15}
Rise Time vs. $FWHM$	0.79	1.3×10^{-40}
Rise Time vs. Area	0.59	3.3×10^{-10}
Rise Time vs. Pulse Amplitude	0.013	0.90
Fall Time vs. $FWHM$	0.75	2.6×10^{-33}
Fall Time vs. Area	0.64	2.0×10^{-12}
Fall Time vs. Pulse Amplitude	0.078	0.45
$FWHM$ vs. Area	0.60	6.89×10^{-11}
$FWHM$ vs. Pulse Amplitude	-0.05	0.64
Area vs. Pulse Amplitude	0.65	1.1×10^{-12}

Table 3. The Spearman correlation coefficients ρ and probabilities for ΔTs (first 2 rows) and PAs (second 2 rows). The first and third rows refer to adjacent ΔTs and PAs while the second and fourth rows refer to ΔTs or PAs separated by one time interval or pulse. The first/second entry for the ΔTs gives ρ when the ΔTs are unnormalised/normalised by T_{90}. The first/second entry for the PAs gives ρ when the PAs are unnormalised/normalised by the maximum peak in the burst.

Total number	ρ	Probability
140	0.42/0.30	$1.7 \times 10^{-12}/3.0 \times 10^{-3}$
84	0.48/0.32	$4.9 \times 10^{-6}/3.2 \times 10^{-3}$
213/107	0.39/0.24	$5 \times 10^{-9}/1.1 \times 10^{-2}$
140/84	0.13/$-$0.09	0.13/0.42

number of long time intervals in excess of 15 s. It was also found that the values of ΔT were correlated over most of the GRBs and up to more than 20 pulses in the GRBs with large numbers of pulses. In short GRBs there is a strong correlation between the values of ΔT and also between the pulse amplitudes (Table 3) but the latter are better correlated in GRBs with $T_{90} > 2$ s. There are remarkable similarities between the statistical properties of the two classes of GRBs. The clear conclusion is that the same emission mechanism accounts for the two types of GRBs. This conclusion is in agreement with a very different analysis of the temporal structure of short GRBs (Nakar & Piran 2001). The external shock model (Dermer & Mitman 1999) has serious difficulties in accounting for GRBs with $T_{90} < 2$ s and with the non-random distribution of correlated time intervals between pulses. The results presented here provide considerable support for the internal shock model (Rees & Mészáros 1994). The internal shock model can account for the results obtained on long and short GRBs provided the cause of the pulses and the correlated values of ΔT can be attributed to the central engine. It has been shown that the time intervals

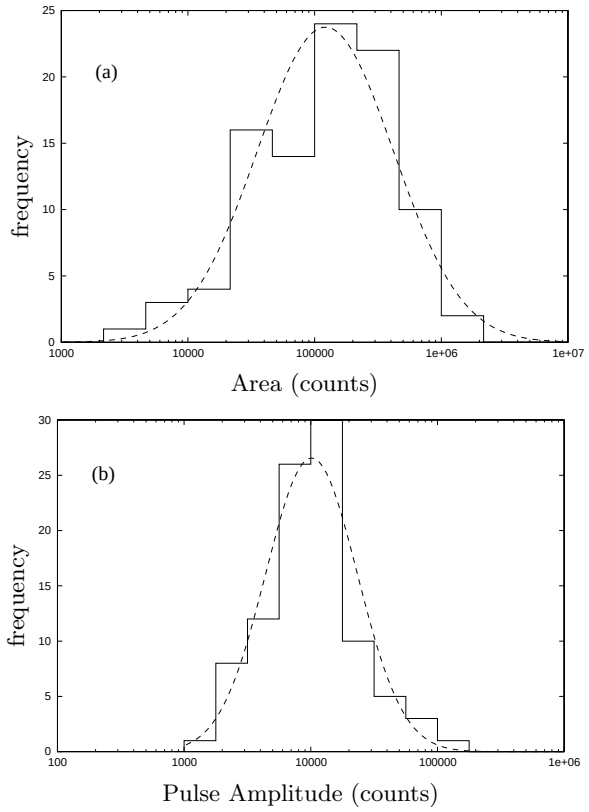

Fig. 3. The distributions of pulse area and amplitude selected at $\tau_\sigma \geq 5$ and $\tau_\mathrm{i} \geq 50\%$ and consistent lognormals (dashed lines). These distributions were generated from 55 GRBs that were summed over two BATSE Large Area Detectors.

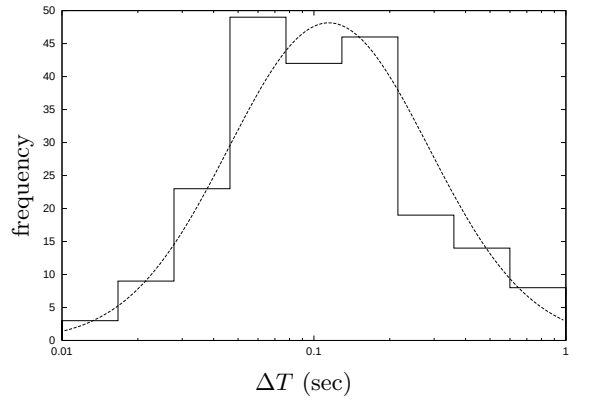

Fig. 4. The distribution of time intervals between the pulses, ΔT, selected at $\tau_\sigma \geq 5$ and consistent lognormal (dashed line).

between glitches in pulsars and outbursts in SGRs are lognormally distributed (Quilligan et al. 2001). The similar distributions of ΔT in short and long GRBs are indirect evidence for rotation powered systems with super-strong magnectic fields.

There is strong evidence that long GRBs originate in star forming galaxies providing evidence that they are linked to massive stars and supernovae (Mészáros 2001). A variety of models, such as collapsars and hypernovae have been proposed as progenitors (e.g. MacFadyen & Woosley 1999). Models of these systems imply that jets can be generated to produce GRBs by an internal shock model. These models cannot account for GRBs with T_{90} less than about 5 s. The shorter GRBs have been attributed to neutron star (NS) – NS mergers or NS – black hole mergers (e.g. Ruffert & Janka 1999). A common ingredient of most GRB models is the formation of a black hole with a temporary torus that accretes and powers the relativistic jets and the GRBs. The overall energetics of the various progenitor models differ by at most an order of magnitude. The GRBs appear to have the same emission mechanism and possibly different progenitors for long and short bursts.

5. Conclusions

A sample of bright GRBs with $T_{90} < 2$ s have been denoised and analysed by an automatic pulse selection algorithm. The results show that the distribution of the properties of isolated pulses and time intervals between all pulses are compatible with lognormal distributions. The same mechanism seems to be responsible for both long and short GRBs and is attributed to the internal shock model.

References

Cline, D. B., Matthey, C., & Otwinowski, S. 1999, ApJ, 527, 827
Dermer, C. D., & Mitman, K. E. 1999, ApJ, 513, L5
Dezalay, J.-P., Barat, C., Talon, R., et al. 1995, Ap&SS, 231, 115
Gupta, V., Das Gupta, P., & Bhat, P. 2000, in CP526, Gamma-Ray Bursts, 5th Hunstville Symposium, ed. R. M. Kippen, et al., 215
Hakkila, J., Haglin, D. J., Pendleton, G. N., et al. 2000, ApJ, 538, 165
Horvath, I. 1998, ApJ, 508, 757
Hurley, K. J., McBreen, B., Quilligan, F., Delaney, M., & Hanlon, L. 1998, in CP428, Gamma-Ray Bursts, 4th Hunstville Symposium, ed. C. A. Meegan, et al., 191
Katz, J. I., & Canel, L. M. 1996, ApJ, 471, 915
Kouveliotou, C., Meegan, C. A., Fishman, G. J., et al. 1993, ApJ, 413, L101
MacFadyen, A. I., & Woosley, S. E. 1999, ApJ, 524, 262
McBreen, B., Hurley, K. J., Long, R., & Metcalfe, L. 1994, MNRAS, 271, 662
Mészáros, P. 2001, Science, 291, 79
Mukherjee, S., Feigelson, E. D., Jogesh Babu, G., et al. 1998, ApJ, 508, 314
Nakar, P., & Piran, T. 2001 [astro-ph/0103192]
Norris, J. P., Scargle, J. D., & Bonnell, J. T. 2000 [astro-ph/0105108]
Paciesas, W. S., Preece, R. D., Briggs, M. S., & Malozzi, R. S. 2001 [astro-ph/0109053]
Quilligan, F., McBreen, B., Hanlon, L., et al. 2001, A&A, submitted
Rees, M. J., & Mészáros, P. 1994, ApJ, 430, L93
Ruffert, M., & Janka, H.-T. 1999, A&A, 344, 573
Schmidt, M. 2001 [astro-ph/0108459]